Alkylated Styrene Ionomers with Variable Length Spacers. 2. Physical Properties

Mario Gauthier† and Adi Eisenberg*

Department of Chemistry, McGill University, Montreal, Quebec, Canada H3A 2K6.
Received March 13, 1989; Revised Manuscript Received August 21, 1989

ABSTRACT: The dynamic mechanical properties of two analogous series of alkylated styrene ionomers were examined. The samples were prepared in the partial base hydrolysis of precursors containing 10–15 mol % of 4-substituted styrene units with substituents R = $-(CH_2)_nCO_2Me$ (n = 1, 5, 10) or R = $-O(CH_2)_nCO_2Me$ (n = 1, 4, 10). The variation in the mechanical properties was studied as a function of ion content for the different ionomers, to yield a systematic investigation of the effects of ion spacing from the polymer backbone. Three distinct factors are postulated as having contributed to the trends observed among the different series of compounds. These include the bulkiness and rigidity of the units to which the ionic groups are attached and the immobilizing effect of the ionic groups on the polymer backbone. Furthermore, in the ether derivatives, the presence of alkyl aryl ether linkages leads to solvation effects and thus reduces clustering.

Introduction

The incorporation of ions into organic polymers has been shown, on occasion, to cause dramatic changes in their physical properties.[1] It is not always clear, however, what are the exact causes for the variations in properties observed between distinct ionomer systems. The systematic variation of the structural characteristics of polymers represents a very valuable way to get some insight into the effects of certain parameters on the physical properties of ionomers. Examples of molecular parameters that were varied in previous studies are the type of counterion,[2] and the placement[3] and nature[4] of pendant ionic groups. More recently, the effects of the matrix polarity and glass transition temperature[5] on ionic aggregation were also examined in styrene ionomers.

The importance of polymer structure variation, and notably of the length of the side chains, is underlined by the industrially important perfluorinated membrane materials.[6] There exists currently several different types of perfluorinated ionomers which are commercially available. Apart from the original sulfonated Nafion products introduced by Du Pont[7] in the early 1970s, another type of perfluorosulfonate membrane material recently developed by Dow[8] has a shorter side chain length than the Nafion products. Analogous carboxylated ionomers are available, among others, from the Asahi Glass Co. (Flemion)[9] and the Asahi Chemical Co.,[10] as well as mixed sulfonate–carboxylate perfluorinated materials (Neoseptа-F) from the Tokuyama Soda Co.[11] Even though the different ionomers were found to operate satisfactorily as membrane materials in the chlor-alkali industry, significant morphological differences were observed between some of them. Comparative studies of these materials to date have been oriented more toward comparing sulfonate vs carboxylate pendant ions,[12] and only to a much smaller extent toward examining the effects of the different chain lengths[13] on the physical properties of the membranes. Even though a study of chain length effects in the perfluorinated ionomers would be of considerable interest, it would be of somewhat limited generality. This is because only very few different types of perfluorinated ionomers are available, and their synthesis is highly involved. Moreover, it has been shown that the degree of crystallinity of these materials depends on different factors such as their ion content.[6] The crystallinity, in turn, would have a profound effect on the mechanical properties of the ionomers.

Ionomers based on styrene have already been the subject of much work. Their amorphous character gives them a distinct advantage over polyolefin ionomers, in that the interpretation of the results is correspondingly simpler. Styrene copolymerizes with a variety of functional comonomers, and the homopolymer can undergo a number of functionalization reactions. For all these reasons, styrene ionomers were preferred over other systems for this work. It is the purpose of the present study to explore the effects of systematic side chain length variation on the dynamic mechanical properties of carboxylated styrene-based ionomers.

One example of previous work dealing with systematic side chain length variation is that of Vogl and coworkers,[14] who reported the synthesis of poly(alkylene oxide)-based ionomers with variable chain length spacers from methyl ω-epoxyalkanoate homopolymers and copolymers with various cyclic ethers and epoxides. Physical properties measurements of interest to the field of ionomers, namely, X-ray diffraction and dynamic mechanical measurements, were limited to very few of the materials prepared. Ionomers derived from ethylene or propylene oxide–methyl 10,11-epoxyundecanoate copolymers were also characterized more recently.[15] The early stages of the investigations done on systematic ion spacing in this laboratory were based on ionomers of styrene–4-hydroxystyrene and styrene–4-hydroxymethylstyrene copolymers.[16]

Some of the problems involved in systematic structure-property relation studies become apparent from the examples given above. The main limitation of such investigations is the difficulty of varying a single structural parameter at a time, without affecting others at the same time; otherwise, the effects observed may not always be clearly assignable to the variation in the parameter of primary interest. Ideally, such a systematic study should be based on the same polymer matrix, with a single, well-defined

* To whom correspondence should be addressed.
† Present address: Institut für Makromolekulare Chemie, Universität Freiburg, Stefan-Meier-Strasse 31, D-7800 Freiburg, Federal Republic of Germany.

0024-9297/90/2223-2066$02.50/0

characteristic used as a variable parameter.

The synthesis of styrene ionomer precursors with methyl alkanoate side chains in the para position and varying in length from 2 to 11 carbon atoms was described in a previous paper.[17] These materials represent an excellent opportunity to examine the effects of the variation of spacing of the ionic groups from the polymer backbone on ion aggregation, and the consequent variations in the mechanical properties of the ionomers. Six different parent (esterified) copolymers were prepared, falling into two distinct families of compounds, according to the mode of attachment of the alkyl chain to the styrene ring. One family (alkyl derivatives) involved the direct attachment of the ω-carboxylated alkyl chain in the para position. In the other family of compounds (ether derivatives), the alkyl chain was attached to the ring through an alkyl aryl ether linkage. This should allow the exploration not only of the ion spacing effects but also of the presence of solvating groups (the ether linkages) on the properties of the resulting ionomers.

The six esterified ionomer precursors prepared were poly(styrene-*co*-4-(carbomethoxymethyl)styrene) [C_2 alkyl], poly(styrene-*co*-4-(5-carbomethoxypentyl)styrene) [C_6 alkyl], poly(styrene-*co*-4-(10-carbomethoxydecyl)styrene)[C_{11} alkyl], poly(styrene-*co*-4-((carbomethoxymethyl)oxy)styrene) [C_2 ether], poly(styrene-*co*-4-((5-carbomethoxypentyl)oxy)styrene) [C_5 ether], and poly(styrene-*co*-4-((10-carbomethoxydecyl)oxy)styrene) [C_{11} ether]. For the sake of simplicity, the nonsystematic names of the compounds, given above in brackets after each systematic name, will be used throughout the rest of this paper. The alkyl derivatives had a pendant carboxyl group concentration of the order of 10 mol % and the ether derivatives, a pendant carboxyl group concentration of approximately 15 mol %. Ionomers of different ion contents were prepared for each series by hydrolysis with a base according to a procedure given here. This approach also ensured that within a given series, only the proportion of ionized groups varied, the rest of the carboxylate moieties remaining as ester groups, thus resulting only in minimal global composition variations. A sample identified as C_2 ether 10% Na would therefore refer to an ionomer derived from the C_2 ether esterified precursor, with 10 mol % of sodium carboxylate moieties and approximately 5 mol % of residual ester groups.

The present work deals with the dynamic mechanical and the differential scanning calorimetry analysis of these ionomers. It is the first of a series of investigations of the physical properties to be performed on these compounds; future work will involve small-angle X-ray scattering measurements and diffusion studies.

Experimental Section

The synthesis of the esterified ionomer precursors was described in a previous paper.[17] A brief summary of the preparation of these materials follows, for the convenience of the reader. The C_2 alkyl ester was prepared via chloromethylation of polystyrene, followed by nucleophilic displacement of the chloride ion by sodium cyanide in a *N,N*-dimethylformamide/water solvent mixture. The nitrile was converted to the methyl ester under mild conditions with methanol/HCl gas via an imino ether hydrochloride intermediate. The C_6 and C_{11} alkyl compounds were similarly prepared from bromoalkylated styrene analogues. These were obtained by lithiation of a styrene–4-bromostyrene copolymer, followed by the addition of a large excess of 1,5-dibromopentane and 1,10-dibromodecane for the C_5 and C_{10} derivatives, respectively. The ether compounds (C_2, C_5, and C_{11} methyl carboxylates) were obtained in a Williamson ether synthesis reaction from a styrene–4-hydroxystyrene copolymer and the corresponding ω-brominated aliphatic acid methyl ester in anhydrous DMF and in the presence of sodium methoxide.

Table I
Description of the Styrene Polymers Investigated and Their Parent Compounds[a]

substituent R	$10^{-3}M_n$, g/mol	$10^{-3}M_w$, g/mol	functionalizatn, mol %
H	66.5	142	
CH_2CO_2Me	52.8	126	9.5
Br	43.5	131	13.8
$(CH_2)_5CO_2Me$	42.6	128	11.4
$(CH_2)_{10}CO_2Me$	50.8	194	11.2
OMe	148	253	15.0
OCH_2CO_2Me	128	294	14.1
$O(CH_2)_4CO_2Me$	161	302	14.8
$O(CH_2)_{10}CO_2Me$	156	320	14.6

[a] The samples are identified according to the substituent R in the para position of the styrene units. The values presented are, from left to right, the number- and weight-average molecular weights (from GPC) and the degree of functionalization of the polymers.

The important characteristics of these materials[17] are summarized in Table I. It can be seen from the data presented that the molecular weight distribution of the polymers, as evaluated by the GPC technique, was not significantly affected by the functionalization processes. The degree of functionalization of the final products, with respect to the parent compounds, is also high (81–98%). In the cases where lower functional yields were obtained (alkyl derivatives), the fraction of groups not converted was also shown to be "inert" (non-ionizable and nonpolar) with respect to this study.[17] The ester groups are distributed randomly along the polymer chain, since the copolymerization reactivity ratio (r_1, r_2) values for the preparation of the parent copolymers were highly favorable.[17]

The esterified polymers were hydrolyzed by refluxing either with sodium hydroxide in a benzene/methanol/water solvent mixture or with sulfuric acid in tetrahydrofuran/water. The acid hydrolysis technique was used to obtain fully hydrolyzed samples of the alkyl series and to check the total carboxylate content of the samples, as previously described.[17] This technique was also used to generate fully ionized samples of the alkyl series. Samples (1.4 g) of the acid-hydrolyzed materials were thus dissolved in 100 mL of 80/20 v/v benzene/methanol and completely neutralized with a predetermined volume of standard 0.05 N methanolic NaOH solution. The ionomers were recovered by freeze-drying.

All other samples used in this study were produced in the base hydrolysis of the esterified polymers. In a typical hydrolysis procedure, 1.3 g of polymer was dissolved in 100 mL of 80/20 benzene/methanol solvent, followed by the addition of 2 mL of water. A calculated amount of standard methanolic 0.05 or 0.10 N NaOH solution, based on the desired ionization level, was then added and the solution refluxed for 3–5 days under nitrogen. Completion of the reaction was confirmed by adding a few drops of a 0.1% phenolphthalein indicator solution in ethanol to a 1-mL sample of the hydrolyzed polymer solution. The solution remained colorless if all the base initially added had been consumed in the reaction; however, it developed a pink coloration upon adding a single drop of a 0.01 N NaOH solution. The partly ionized polymer was recovered by freeze-drying. Samples with the ion contents given in Table II were prepared by using either the complete acid hydrolysis–neutralization (alkyl series, ca. 10 mol % ions) or the direct base hydrolysis scheme described above (other samples). The total carboxylate content of the parent (esterified) ether polymers, as determined by titration of the acid-hydrolyzed materials, was about 14.5 mol %.

The extent of ionization of the samples was also confirmed by NMR analysis of some of the products. The ratio of the integrated intensities of the methoxy peak (δ = 3.7–3.8 ppm) to the aromatic peaks (δ = 6.2–7.6 ppm) of a partly hydrolyzed sample thus showed a decrease, compared to the esterified polymer, which was proportional to the extent of hydrolysis.

Differential scanning calorimetry (DSC) was used to determine the glass transition temperature of the samples. A Perkin-Elmer DSC-2C instrument was used for this purpose. Calibration was achieved with indium and tin standards. Each sam-

Table II

material	EW, g/mol	DSC T_g, °C	matrix T_g, °C	$W_{1/2}$, °C	clust T_g, °C	$W_{1/2}$, °C	$E'_{in.}$	$T_{in.}$, °C	M_c, g/mol	$-E_a$(ma), kJ/mol	r^2	$-E_a$(cl), kJ/mol	r^2
C_2 alkyl ester		105	114	13			7.9E+05	156	14240	482	0.9995		
C_2 alkyl 2.5% Na	4220	115	126	15	167	17	3.1E+06	151	3559	470	0.995	232	0.993
C_2 alkyl 5% Na	2150	127	136	15	179	31	7.3E+06	156	1549	496	0.998	246	0.998
C_2 alkyl 7.5% Na	1450	131	142	19	178	20	7.4E+06	164	1557	553	0.990	250	0.995
C_2 alkyl 9.5% Na	1110	145	151	18	226	68	1.5E+07	174	785	589	0.9997	186	0.998
C_6 alkyl ester		81	94	14			5.0E+05	122	20605	413	0.996		
C_6 alkyl 2.5% Na	4280	86	102	16	195	35	1.1E+06	144	10412	434	0.997	990	1.0000
C_6 alkyl 5% Na	2200	100	115	15	183	53	2.7E+06	137	4051	458	0.995	175	0.95
C_6 alkyl 7.5% Na	1510	113	127	17	187	47	4.8E+06	149	2282	503	0.994	202	0.998
C_6 alkyl 11.4% Na	1160	133	139	21	201	31	1.6E+07	160	704	580	0.997	464	0.97
C_{11} alkyl ester			78	18			2.8E+05	111	36300	321	0.9999		
C_{11} alkyl 5% Na	2270	85	100	18	136	25	6.1E+06	123	1690	395	0.991	258	0.995
C_{11} alkyl 7.5% Na	1580	102	117	19	166	49	1.4E+07	135	792	474	1.0000	193	0.997
C_{11} alkyl 11.2% Na	1230	131	132	25	184	32	2.6E+07	155	428	561	0.997	561	0.997
C_2 ether ester		96	108	15			2.4E+05	142	44900	472	0.9999		
C_2 ether 5% Na	2260	114	122	21	160	26	2.4E+06	181	4910	439	0.996	233	0.990
C_2 ether 7.5% Na	1470	118	131	29	171	19	4.3E+06	188	2790	422	1.0000	200	0.996
C_2 ether 10% Na	1120	139	152	33	184	20	6.7E+06	199	1846	739	0.9990	297	0.994
C_2 ether 14% Na	830	169	172	18	203	23	1.4E+07	212	894	646	0.993	366	0.990
C_5 ether ester		80	94	15			3.3E+05	124	31700	432	0.9996		
C_5 ether 5% Na	2200	99	108	16	148	40	1.1E+06	178	10700	434	0.995	258	0.9996
C_5 ether 7.5% Na	1510	104	116	19	162	39	3.0E+06	148	3630	395	0.996	220	0.996
C_5 ether 10% Na	1160	113	125	19	171	36	4.9E+06	152	2290	502	0.9990	272	0.9999
C_5 ether 14% Na	870	156	139	18	180	29	1.7E+07	156	646	562	0.998	229	0.9992
C_{11} ether ester			71	17			1.7E+05	110	58300	319	0.990		
C_{11} ether 2.5% Na	4370	66	82	18	130	27	1.6E+06	110	6120	338	0.990	171	0.995
C_{11} ether 5% Na	2290	78	92	18	138	28	4.9E+06	116	2090	367	0.997	196	0.998
C_{11} ether 7.5% Na	1590	89	104	21	146	22	1.5E+07	128	696	379	0.997	224	0.993
C_{11} ether 10% Na	1250	101	115	23	173	42	2.7E+07	140	399	444	0.998	250	0.994
C_{11} ether 14% Na	950	133	140	19	197	41	5.4E+07	157	211	689	0.995	518	0.997

ple was initially heated to ca. 40 °C above the T_g of the material for 5 min, followed by quenching at the maximum rate attained by the instrument. Duplicate scans at 20 °C/min were used to insure reproducibility of the results. The agreement between two successive runs was generally better than 1 deg.

The samples for dynamic mechanical analysis were dried under vacuum at 100 °C for 14–17 days prior to molding. The mold was preheated at 180–240 °C (depending on the matrix T_g of the sample) before transferring the dried material; a pressure of 20 MPa was maintained for 10 min at the desired temperature. The pressure was then very slowly released and the mold was allowed to cool down on the press to ca. 10 °C below the matrix T_g of the material as determined from DSC measurements. The sample was taken out of the mold and used immediately for the dynamic mechanical measurements. Approximate sample dimensions were 2.5 mm thickness × 12 mm width × 36 mm length. These mechanical measurements were done by using a Polymer Laboratories Mark II dynamic mechanical thermal analyzer (DMTA) in the dual cantilever bending mode, at frequencies of 1, 3, 10, and 30 Hz and a heating rate of 0.5 °C/min. The furnace of the instrument was continuously purged with a flow of dry nitrogen throughout the run.

In view of the cross-linking effects observed in the samples (particularly in the ether compounds), an infrared study of the nature of thermal degradation was attempted for the C_{11} ether 10% Na sample. Films were prepared for infrared spectroscopy by compression molding of 0.1 g of the ionomer between plates covered with aluminum foil. In one case, a film was obtained by molding the sample only for a few minutes at 200 °C.. In another case, the same material was maintained at 275 °C for 5 h. Infrared spectra were recorded for both films by using an Analect AQS-40 FT-IR spectrometer with a resolution of 4 cm^{-1}.

Results

In the dynamic mechanical analysis, the storage modulus, loss modulus, and loss tangent of each sample was obtained as a function of temperature at four different frequencies. Because of the similar behavior for the different series, only representative results will be given here in graphical form. Figure 1 shows the storage modulus curves obtained for the C_{11} ether series, for ion concentrations varying from 0 to 14 mol %. Because of slight scatter observed in the data (maximum log E' variations ±0.06), the absolute values of the glassy moduli were adjusted, for ease of comparison, to the average of all

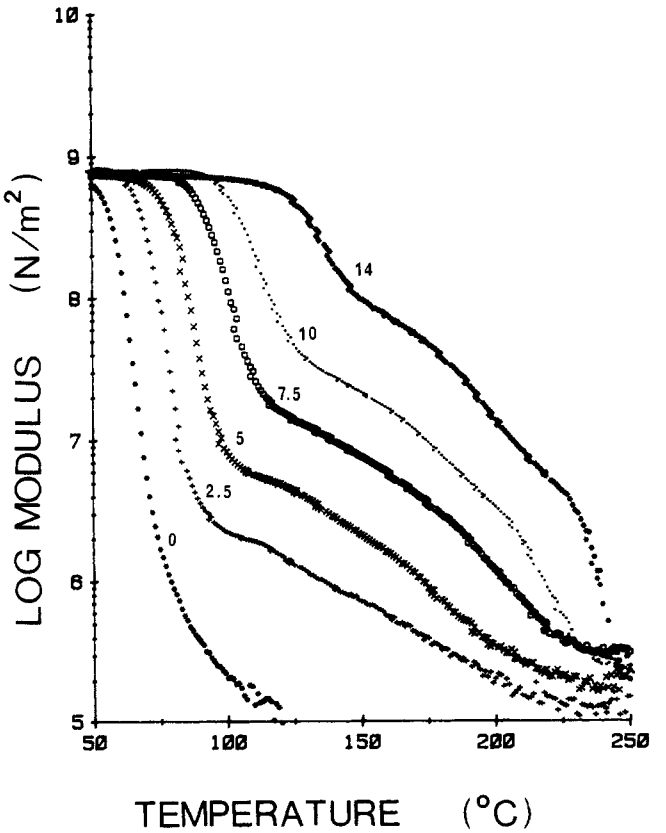

Figure 1. Dynamic storage modulus curves (1 Hz) for the C_{11} ether series; ion contents vary from 0 to 14 mol %, as indicated.

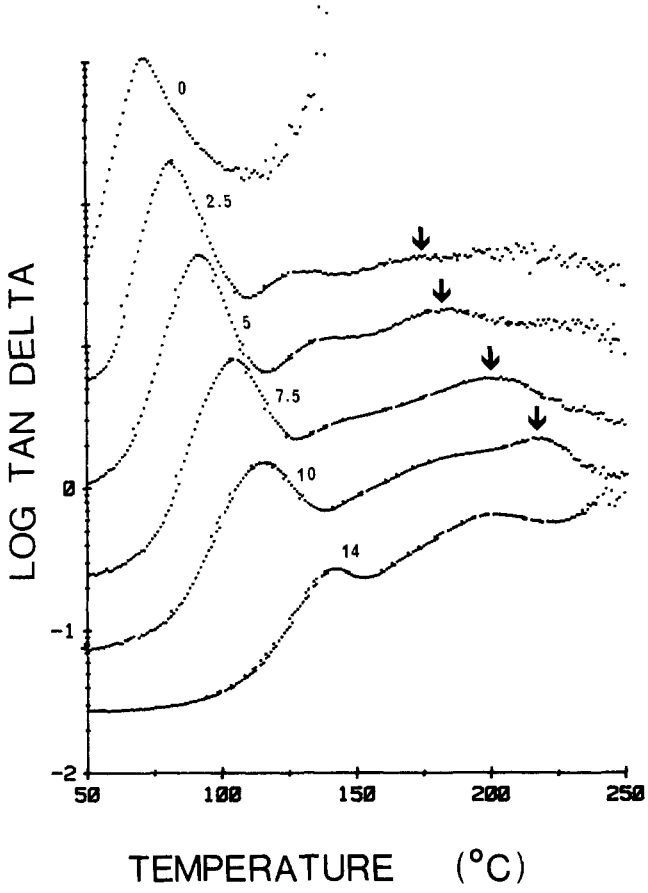

Figure 2. Loss tangent curves (1 Hz) for the ionomers of Figure 1. The scale indicated is correct for the bottom curve; each successive curve is shifted up by a half order of magnitude with respect to the previous one, for improved clarity.

the samples (8.90×10^8 Pa at 35 °C). The corresponding loss tangent curves are given in Figure 2. It can be seen that the general features of the system correspond to what has already been observed in other clustered styrene ionomers such as polystyrene-*co*-sodium methacrylate.[18] The features of interest include a 70 °C increase in the matrix glass transition temperature and a large increase (ca. 2.5 orders of magnitude) in the ion-associated rubberlike modulus over the ion concentration range studied (0–14 mol %). The position of the rubberlike plateau is also shifted toward higher temperatures. At the same time, the height of the first loss tangent peak (matrix) decreases in favor of the second (cluster) peak with increasing degree of ionization.

The somewhat different results obtained for the C_2 ether series are presented in Figure 3, for comparison. It can be seen that the height of the ion-associated rubberlike modulus of these samples is significantly lower than for the corresponding C_{11} ether samples. As before, the absolute value of the glassy modulus was adjusted to the average value of all samples (log E' = 9.18 at 35 °C; maximum variations +0.09 and −0.14).

One special feature of the tan δ vs temperature curves (Figure 2) is, however, the presence of a third, high-temperature loss peak (indicated by arrows in Figure 2), in contrast with the two normally observed for amorphous clustered styrene ionomers.[18] In fact, the presence of a third peak is characteristic of most of the systems studied here. It will be shown later that the third peak is attributable to cross-linking of the samples occurring in the course of the DMTA run at high temperatures. The presence of this third peak will therefore be neglected in the subsequent interpretation of the results. The modulus increase toward the end of the runs (starting around 225 °C for the C_{11} ethers, as shown in Figure 4, and at about 250 °C for the C_2 ethers) is another manifestation of cross-linking in that temperature range.

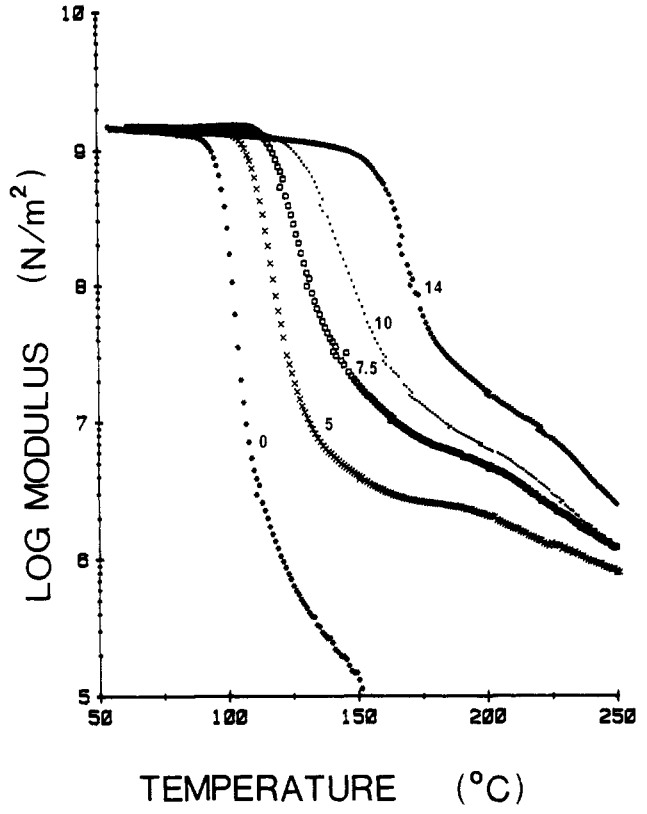

Figure 3. Dynamic storage modulus curves (1 Hz) for the C_2 ether series; ion contents (mol %) are as indicated.

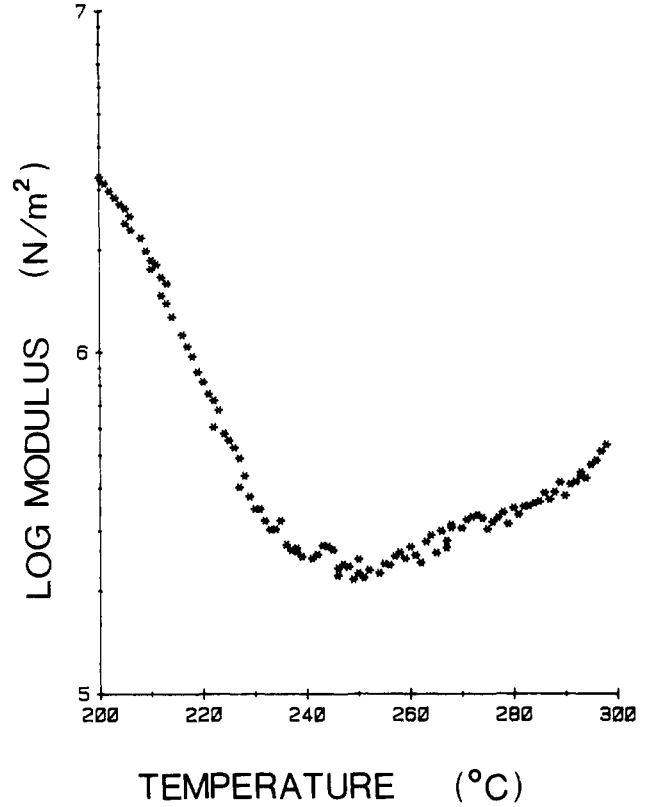

Figure 4. Storage modulus increase of the C_{11} ether 10% Na sample in the 200–300 °C range.

The dynamic mechanical curves were numerically analyzed on an IBM-XT compatible personal computer to extract all the useful information using a previously described program.[5] The information thus obtained includes the position and width at half-height of the peaks in the tan δ curves, the magnitude of the ion-related rubberlike inflection modulus, and the corresponding temperature in the storage modulus curves, as well as the activation energies calculated from the frequency shift of the tan δ maxima. These are summarized for each sample in Table II. This presentation format was preferred for the results over a graphical approach because of the quite distinct behaviors observed in comparing the different series with each other. The glass transition temperatures determined by DSC analysis are also included for comparison.

The values presented are the ion content (mol %) and equivalent weight (EW) of the samples, the T_g determined by DSC [T_g(DSC)], the 1-Hz matrix and cluster T_g [T_g(ma) and T_g(cl), respectively], and their corresponding widths at half-height ($W_{1/2}$). Also included are the values of the inflection modulus ($E'_{in.}$) and temperature ($T_{in.}$) as well as the calculated activation energies of the matrix [E_a(ma)] and cluster [E_a(cl)] peaks, with the corresponding correlation coefficients (r^2). The experimental average molecular weight between cross-links (M_c) was calculated for each sample from the corresponding inflection modulus and temperature.

The cross-linking efficiency of the ionic aggregates may be expressed as the ratio M_c(cal)/M_c(exp), where M_c(cal) is the theoretical value calculated for strictly multiplet-type interactions and is equal to the equivalent weight of the sample; M_c(exp) is the average molecular weight between cross-links determined from the observed rubberlike modulus. This is illustrated in Figure 5 for the different alkyl and ether series compounds. These are compared to data obtained for styrene–sodium methacrylate[19] and styrene–sodium 4-styrenecarboxylate ionomers.[20]

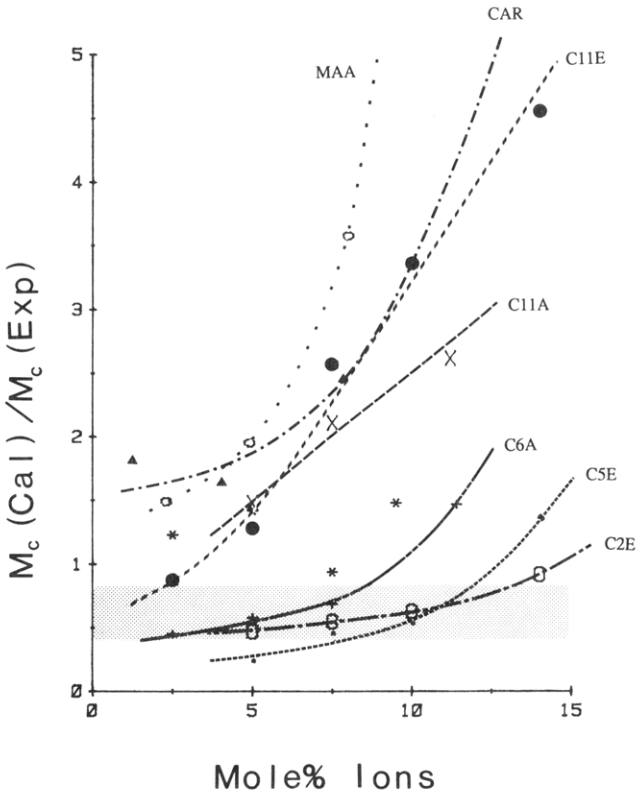

Figure 5. Comparison of the cross-linking efficiency of the ionic aggregates in the different families of sodium ionomers. The experimental points and the corresponding curves are identified: * (no curve), C_2 alkyl; +, C6A, C_6 alkyl; ×, C11A; C_{11} alkyl; o, C2E, C_2 ether; ·, C5E, C_5 ether; ●, C11E, C_{11} ether; o, MAA; methacrylic acid;[19] △, CAR, carboxylated polystyrene.[20]

Table III
dT_g/dC by DSC and from Dynamic Mechanical Data (Matrix and Cluster Peaks)[a]

	DMTA		
series	matrix	clusters	DSC
C_2 alkyl	3.6 ± 0.2	8.7 ± 0.8	4.0 ● 0.3
C_6 alkyl	4.1 ± 0.2	2.9 ± 0.3	4.7 ± 0.3
C_{11} alkyl	4.9 ± 0.2	8 ± 1	
C_2 ether	4.7 ± 0.4	4.8 ± 0.1	4.0 ± 0.5
C_5 ether	3.2 ± 0.1	3.5 ± 0.4	3.2 ● 0.2
C_{11} ether	4.8 ± 0.2	6.0 ± 0.6	4.6 ± 0.1

[a] The values and uncertainties given were obtained by least-squares fit of the data; the units are °C/mol %.

Discussion

The following order will be used to discuss the experimental observations. The variation of the matrix T_g with ion concentration will be discussed first because it is least sensitive to cross-linking effects under the conditions used. The experimental evidence for network formation and the reasons for ascribing the third loss maximum to chemical cross-linking will then be considered. This clarification will lead to a discussion of the observed variation with ion concentration of the cluster-related glass transition temperatures as well as of the activation energies associated with both the matrix and cluster T_g's. The discussion will be concluded by the consideration of the different molecular parameters thought to be responsible for the observed effects.

Matrix Glass Transition Temperature. An examination of the data in Table II reveals a monotonic increase in the matrix T_g with ion content (dT_g/dC), as measured by both the DSC and the DMTA techniques. This is generally associated with a decrease in segmental mobility due to ionic aggregation.[21] The different slopes obtained for all six systems are given in Table III for comparison. In the dT_g/dC calculations for the ether series obtained by DSC, the data for the 14% samples was excluded. It is generally accepted that as the ion content of the samples increases, the width of the transition region of DSC scans increases as a result of contributions from both the matrix- and the cluster-related glass transitions. This effect resulted in a significant deviation from linearity at 14% ion content. No calculations were performed for the C_{11} alkyl samples analyzed by DSC because only three data points were available for the analysis and showed considerable scatter (Table II). The discussion of the data for the T_g associated with the ion-rich domains (clusters) will be postponed to a later stage. Both the DSC and the DMTA techniques show a clear tendency for dT_g/dC to increase along the series C_2 alkyl < C_6 alkyl < C_{11} alkyl. However, no significant trend is observed for the ether series. In particular, the dT_g/dC values calculated for the C_5 ether derivatives are unexpectedly low. The following distinctions can be made concerning the two families of compounds. In the alkylated ionomers, the degree of functionalization is about 10–11 mol %; the ether compounds, however, have a pendant group concentration of ca. 15 mol %. Otherwise, the only difference between the two families concerns the mode of attachment of the pendant alkyl chain to the rings, namely, the presence of an alkyl aryl ether linkage in the case of the ether analogues. The

slightly higher concentration of ester groups in the ether than in the alkyl series appears to be an unlikely cause for the different tendencies observed. The lack of trends in the ether analogues could therefore be related to the ion-solvating properties of ethers.[22] Even though solvation effects due to ester functionalities have been linked to their somewhat different aggregation behavior[23] compared to styrene ionomers, they do not seem to cause a significant change in the dT_g/dC value: poly(ethyl acrylate-*co*-sodium acrylate) (3.4 °C/mol %)[23] compares to poly(styrene-*co*-sodium 4-styrenecarboxylate)[20] (2.7 °C/mol %), poly(styrene-*co*-sodium 4-styrenesulfonate) (4 °C/mol %[24] or 3.3 °C/mol %),[25] and sodium ionomers of poly(styrene-*co*-4-hydroxystyrene)[16] (3.2 °C/mol %).

Apart from the T_g increase with the ion content of the samples, the T_g differences observed between the different families of ionomers (Table II) show the expected variations of plasticized systems. Thus, between the different alkyl or ether compounds, for identical ion contents, the longer the attached chain, the lower the T_g of the sample. The T_g of the ether compounds is also lower than those in the corresponding alkyl series presumably because of the higher degree of substitution of the ether derivatives (15 mol %) compared to the alkyls (10 mol %).

Similar trends are observed in both the dynamic mechanical and the DSC data, the two sets of curves being essentially parallel. There is, however, a systematic difference of ca. 10–15 °C between the two techniques, which becomes slightly larger for the longer chain lengths. This is attributed to the frequency effect of the dynamic mechanical experiments. It seems reasonable, however, that the larger samples (ca. 1.3 g) used in the dynamic mechanical experiments may also cause a slower thermal response of the material, even though the scanning rate is also slower in that case (DMTA, 0.5 °C/min; DSC, 20 °C/min).

Cross-Linking Effects. It was mentioned previously that three loss peaks were observed in the tan δ–temperature curves obtained by dynamic mechanical analysis of most samples. Obvious hints of the occurrence of cross-linking during the DMTA runs could be observed. These included, among others, the increase in the storage modulus with temperature in the upper temperature range (Figure 4), as well as the lack of sample flow. A second run performed on the same sample displayed an increased matrix T_g (first run, T_g = 115 °C; second run, T_g = 131 °C at 1 Hz). All ionic samples were insoluble after the DMTA runs; the nonionic esters, which were heated only to lower temperatures, however, remained soluble.

The cross-linking phenomena observed seemed to be more important for the ether than the alkyl compounds. Comparison of IR spectra of the 10% hydrolyzed C_{11} ether compound before and after prolonged heating showed no clear hints concerning the nature of the reactions involved in the cross-linking process. It is suspected that the ether derivatives may undergo a thermal rearrangement reaction analogous to those reported for certain alkyl aryl ethers at elevated temperatures (200–350 °C)[26] to yield, among others, alkylated phenols. The process is known to involve free radicals, at least to some extent, which could explain the greater tendency observed for the ether than for the alkyl derivatives to cross-link. This possibility is supported by the lack of significant changes in the IR spectra before and after heating, already pointed out above. Considering the low concentration of ether linkages (15 mol %), it seems reasonable that the thermal rearrangement of a fraction of the ether groups in these polymers does not result in easily detectable changes. The fact that the carbonyl band (1750 cm^{-1}) remains unchanged in both intensity and shape also rules out the occurrence of a decarboxylation reaction.

The effects of "dynamic cross-linking" (network formation during the course of a thermal scan experiment) on the dynamic mechanical properties of epoxy resins are well-known and have been the subject of a number of papers.[27,28] Of particular relevance to this work is the frequent appearance of an extra dispersion in the loss tangent–temperature curve of uncured or partially cured systems. Lee and Goldfarb[28] suggested considering the observed dynamic modulus (G or E) of curing systems as resulting from two distinct contributions, due to thermal and curing effects, respectively. The response of a sample in a temperature scan experiment may therefore be expressed as a function of these two parameters as

$$\frac{dG(n,T)}{dt} = \left[\frac{dG}{dn}\right]_T \frac{dn}{dt} + \left[\frac{dG}{dT}\right]_n \frac{dT}{dt} \qquad (1)$$

where n is a loosely defined cure parameter such that $n = 0$ for an uncured sample and $n \to \infty$ for complete curing and T is the experimental temperature. The main implication of eq 1 is that the observed modulus may be expanded into an isothermal curing contribution (first term) in addition to the conventional thermal scan contribution (second term). The relation described by eq 1 may be further simplified by assuming that the extent of cure of the system can be described by the increase in T_g in the form of a reduced parameter $(T - T_g)$

$$\frac{dG}{dT} = \frac{dG}{d(T - T_g)}\left[\frac{dT}{dt} - \frac{dT_g}{dt}\right] \qquad (2)$$

where dT/dt and dT_g/dt describe the thermal and the curing effects, respectively.

The actually observed response depends on the magnitude of each of the terms of eq 2. The authors distinguished four different possible cases for a temperature scan experiment. Type I behavior corresponds to $dT_g/dt = 0$, i.e. no curing contribution, giving rise to the response normally observed for thermoplastics in the absence of curing or for fully cured thermoset systems. For $dT/dt > dT_g/dt \neq 0$ (stage II), $(T - T_g)$ is an increasing function, since the T_g change due to curing is small with respect to the time scale of the experiment. Stage III is identified by the condition $dT/dt < dT_g/dt$. This corresponds to a fast curing rate on the time scale of the experiment, and $(T - T_g)$ becomes a decreasing function. Finally, stage IV ($dT_g/dt < 0$) is seldom observed and can be related to polymer degradation or the absorption of diluent by the sample.

This stage description approach was used by the authors to qualitatively describe the dynamic curing of different types of epoxy resin systems. It is suggested that the same approach may be used to describe the cross-linking effects observed in the polymers of interest to the present study. However, it should be kept in mind that since the covalent cross-link density involved in this case is significantly lower than for high-temperature epoxy resins, the features observed are correspondingly less pronounced. For the purpose of the discussion, the behavior of the C_{11} ether 10% Na sample will be considered. It is assumed that the rate of cross-linking is negligible on the time scale of the experiment at the lower temperature range (T < 175–200 °C), corresponding to a type I behavior. This assumption is based on the observation that all the nonionic (esterified) samples of the poly-

mers analyzed by the DMTA technique up to that temperature range remained soluble. Likewise, the salt heated for short periods (ca. 1 h) at 200 °C also remained soluble. The features observed for this part of the curve are typical of carboxylated ionomer systems: increased matrix T_g, high rubberlike modulus, appearance of a second loss tangent peak (Figures 1 and 2). At temperatures between 175 and 250 °C, however, there are two successive changes in slope of the storage modulus curve (Figure 1, 10 mol % curve), rather than the simple flow behavior usually observed. At around 250 °C, the modulus curve flattens, before increasing in a nonlinear fashion from 250 to 300 °C (shown in Figure 4). Calculations for the cross-linking density from rubberlike elasticity ($E = 3\rho RT/M_c$) have shown that the rate of increase of E' with the temperature is much more than expected for a "static" cross-linked system in the 250–330 °C range. Considering also the lack of significant sample deformation, this increase was attributed to "dynamic" cross-linking occurring during the course of the experiment. The fact that the position of the third loss maximum is shifted upward on the temperature scale (Figure 2) with the degree of ionization of the sample suggests that the cross-linking rate may be diffusion-controlled, being more limited in samples where ionic aggregation is more extensive because of the increased sample viscosity.

According to the Lee and Goldfarb model, the increase in modulus would be a result of the occurrence of a stage III condition ($dT/dt < dT_g/dt$), which is equivalent in a way to retracing the modulus curve from right to left.[28] The occurrence of a stage II condition ($dT/dt > dT_g/dt$) has to be assumed because the system necessarily has to go through it to reach the stage III condition. Both stages II and III result in the increased T_g observed in the second scan (ΔT_g = 16 deg). The overall behavior of the present ionomers may therefore be described as being of type I–II–III.

Independently of the justifications brought by the stage description approach, other arguments may be used to warrant discarding the third loss peak as a dynamic cross-linking effect. The temperature of the second (cluster-related) loss maximum falls in a range typical of other carboxylated styrene ionomers (e.g. styrene–sodium methacrylate,[18,19] styrene–sodium 4-styrenecarboxylate[20]), if the plasticizing effect of the pendant alkyl chains is taken into consideration. This is particularly worth noting at the lower ion contents (2.5–7.5%), where the second tan δ peak is at a much more reasonable position than the cross-linking peak, which occurs only approximately 50 deg higher. Furthermore, the variation in the relative intensities of the first (matrix) and the second (cluster) loss maxima follows the pattern usually observed for increasing ion contents, the second peak becoming clearly dominant in the 10–14 mol % interval (Figure 2).

All the factors mentioned above are believed to justify the assignments made for the loss tangent–temperature peaks, namely, associated with the matrix, clusters, and "dynamic cross-linking", from the low- to the high-temperature range, respectively.

Cluster-Related Glass Transition Temperature. It was mentioned earlier that because of the proximity of the cross-linking peak to the cluster peak in the tan δ–temperature curves, it was necessary in many cases to "deconvolute" the peaks with the help of a numerical analysis procedure described elsewhere.[5] Because of the somewhat empirical character of base-line selection and the broader peaks associated with the ion-rich (cluster) domains, the results are expected to be less reliable than for the matrix peak. In the case of the sharper matrix peaks, variations of the order of 1 deg were obtained by intentionally selecting different possible base lines. For the cluster peaks, however, variations of the order of 2–3 deg were observed in the same conditions. Not surprisingly, the cluster peak positions show more scatter than the matrix peaks and approximately linear increases with ion contents (Tables II and III) and dT_g/dC values ranging from approximately 3 to 9 °C/mol. No significant trend seems to emerge from a comparison of the different series (Table II).

Activation Energies. It can be seen in Table II that the activation energy of the matrix-related transition increases with the ionic group concentration and tends to be higher for the alkyl than for the ether derivatives. The matrix activation energies are also highest for the shorter chain compounds. The cluster-related activation energies show a similar trend; also, more scatter is present. Some experimental results were rejected (Table II) on the basis of abnormal loss peak shapes within a run. The overall average trends for the activation energies may be represented (in kJ/mol) as a function of the ion concentration C (in mol %) by

$$E_a(\text{ma}) = (15 \pm 3)C + (380 \pm 20) \quad (3)$$

and

$$E_a(\text{cl}) = (7 \pm 3)C + (180 \pm 20) \quad (4)$$

for the matrix- and cluster-related transitions, respectively. The fact that the cluster-related activation energy is significantly lower than that associated with the matrix has been suggested[19] as providing strong support to the presence of two distinct phases (the ion-poor matrix and the ion-rich clusters) as detected by dynamic mechanical analysis. It was pointed out that if a single phase were present in the system, a dispersion occurring at a higher temperature should have a higher activation energy.

However, one word of caution is necessary, in that the magnitude of the uncertainties associated with the activation energies is rather large. It was explained earlier that the accuracy of the values of the matrix- and cluster-related loss maxima were expected to be of the order of 1 and 2–3 deg, respectively. The "relative" variations expected within a set of curves for a given sample at the different frequencies were, however, expected to be significantly smaller. This is because the curves obtained at the different frequencies are essentially identical in shape. Consequently, it is possible to set the base line in a virtually identical manner within a set of curves. The variations thus expected for the matrix and cluster peak positions were arbitrarily set to 1/3 of the values given above, leading to uncertainties of the order of 0.3 and 0.7–1.0 deg, respectively. Even though this 1/3 factor is of a very empirical nature, it proved to be consistent with the variations observed in the data. The resulting uncertainties in the temperature were included in the linear regression calculations[29] used to obtain uncertainties in the calculated activation energies. Typical errors for the matrix- and cluster-related activation energies were of about 50 and 100 kJ/mol, respectively.

Factors Affecting Ionic Aggregation. The aggregation efficiencies of the ions in the different ionomer series were presented as a function of the ionization level in Figure 5. As explained earlier, the $M_c(\text{cal})/M_c(\text{exp})$ ratio was used for this purpose. The advantage of this approach is that it provides a simple way of comparing the effect of ionic aggregation in the samples with respect to a reference state. This reference state is a system in

which all ion pairs are interacting in the form of multiplets only [M_c(cal)], in the absence of cluster structures. This M_c value also corresponds to the equivalent weight of the sample. A ratio greater than one (experimental M_c < calculated M_c) implies an enhanced state of aggregation, likely in the form of large-scale ionic aggregation (clustering). In contrast, a ratio of less than unity points at a reduced state of aggregation. However, because the determined M_c(exp) result from the average effect of all the ionic aggregates present in the samples, M_c(cal)/M_c(exp) < 1 does not necessarily exclude the presence of clusters but is rather indicative of a reduced state of clustering, when compared to a system with a larger ratio.

Several clear-cut trends emerge from Figure 5. It can be seen that at low ion concentrations, most samples fall in or extrapolate to a band of M_c(cal)/M_c(exp) = (0.6 ± 0.2), showing that the cluster structures, if present, are not rheologically significant. Multiplet formation, therefore, seems to dominate at low ion concentration in most samples. The onset of deviation from that behavior, as well as the trends at high ion contents, however, are a function of the type of compound involved. The following trend in the ratio is observed for deviations outside the (0.6 ± 0.2) band described above:

$$C_2 \text{ ether} < C_5 \text{ ether} < C_6 \text{ alkyl} < C_{11} \text{ alkyl} \approx C_{11} \text{ ether}$$

It can be noticed from Figure 5 that the C_{11} alkyl and the C_{11} ether series display very similar characteristics. This seems reasonable, considering the length of the alkyl chain (10 methylene units) separating the ionic groups from the styrene rings in both cases. For the same reason, the presence of an ether linkage does not seem to influence significantly the aggregation behavior of those samples. On the other hand, the C_2 ether and the C_5 ether series also behave very similarly. The C_6 alkyl derivatives display aggregation characteristics that are intermediate between these two groups. The results for the C_2 alkyl compounds, however, cannot be explained and will not be discussed here at great length. It is suspected that the higher matrix and cluster T_g's observed in these compounds may have led to a merging of the cluster and thermal cross-linking loss tangent peaks, making it impossible to separate the two effects.

In order to rationalize the observed variations in the dynamic mechanical properties of the ionomers presently studied, it seemed reasonable to postulate the existence of three distinct factors affecting the ionic aggregation. These are the bulkiness and rigidity of the units to which the ionic groups are attached, the efficiency of the pendant ionic groups in immobilizing the polymer backbone, and, finally, in the case of the ether compounds, the presence of solvation effects due to the alkyl aryl ether linkages.

In consideration of the last factor, it is possible to argue that the C_2 and C_5 ether derivatives are less clustered than the C_6 alkyl series because of the presence of the solvating oxygen atom linking the relatively short alkyl chain to the styrene ring. Because of their shorter chain length, the incorporation of these ionic groups into the cluster structures also brings along solvating groups (the ether linkages), which may lead to a less favorable ion–ion interaction energy than in their absence. This solvation factor could also explain why the C_6 alkyl series is significantly more clustered than the C_5 ether at the higher (10–11 mol %) ionization level, the total chain length being otherwise identical (six atoms in both cases). The somewhat increased state of aggregation of the C_5 ether 14% Na sample compared to the C_2 ether 14% Na sample could also be taken as indicative of more important solvation effects in the latter case. As mentioned before, the very similar behaviors of the C_{11} alkyl and the C_{11} ether series compounds could be related to the increased distance between the solvating ether linkage and the ionic chain end. The fact that the characteristics of the different series become more easily distinguishable in the higher ion concentration range is not surprising as such, since it is known that the extent of clustering is greatly enhanced in styrene ionomers at ion concentrations above 6–7 mol %.[18]

It was already pointed out that the C_5 ether 14% Na sample displays a somewhat increased state of aggregation (Figure 5) relative to the analogous C_2 ether compound. Apart from the solvation effect postulated above, it seems that the increased local bulkiness (proximity of the styrene ring) of the C_2 relative to the C_5 ether compound may have contributed to the difference in aggregation. The factor involved in this case is the greater proximity of the stiff, bulky styrene ring for the C_2 than for the C_5 ether ionomers, making the incorporation of the bulkier, shorter side chains structures in the clusters energetically less favorable. This factor apparently becomes negligible in the case of the C_{11} compounds presumably again because of the increased distance between the ionic groups and the bulky styrene rings. This is probably why the C_{11} compounds show the most efficient clustering.

The comparison of the present ionomers with previously studied systems highlights the effect of what is thought to be the effectiveness of the pendant ions in immobilizing the polymer backbone. Two additional curves are shown on Figure 5 for comparison, namely, for poly(styrene-*co*-sodium methacrylate)[19] and for poly(styrene-*co*-sodium 4-styrenecarboxylate).[20] The results are directly comparable in the former case because the samples were also studied by using DMTA, i.e. at a constant frequency. The carboxylated styrene analysis was done by using a torsion pendulum, whose oscillation frequency varies with the stiffness of the sample; a bit more caution may therefore be necessary in that case. Once again, it is worth mentioning that the behavior of the 4-carboxystyrene ionomers is qualitatively quite similar to that of the C_6 and C_{11} alkyl compounds, but the C_2 alkyl series does not fit at all, justifying the omission of these results from this part of the discussion.

The styrene–sodium methacrylate ionomers display the characteristics of a most highly clustered system, with a M_c(cal)/M_c(exp) ratio increasing very rapidly above ion concentrations of about 8 mol %. This contrasts with the *p*-carboxystyrene system and obviously even more with the ionomers prepared for this study. More specifically, the comparison of the C_{11} alkyl and ether derivatives with the styrene–sodium methacrylate polymers suggested the importance of the chain immobilization effect. Indeed, it appears that in both cases, local bulkiness alone is not a primary factor determining ionic groups aggregation. The incorporation of a sodium methacrylate unit in a cluster structure is, however, expected to have a more strongly immobilizing effect on the polymer backbone compared to that of carboxylate ion at the end of a long, highly flexible alkyl chain. It seems that the aggregation of sodium methacrylate units, even though energetically approximately as favorable as for the alkylated ionomer, drags more organic material from the polymer backbone into the cluster, possibly leading to a larger overall cluster size, compared to the alkylated compound.

Conclusions

It was shown that the incorporation of ionic group spac-

ers of variable chain length resulted in significant variations in the dynamic mechanical properties of carboxylated styrene ionomers. The results were compared, among others, in terms of ratios $M_c(cal)/M_c(exp)$, where $M_c(cal)$ represents the calculated molecular weight between cross-links, assuming strictly multiplet-type interactions, and $M_c(exp)$ is the experimental molecular weight between cross-links evaluated from the value of the inflection modulus of the ion-related rubbery plateau. All the experimental cross-link densities determined were significantly lower than for other previously characterized highly clustered systems, such as poly(styrene-*co*-sodium methacrylate). Three distinct factors were postulated as contributing to the variations in properties observed among the different series. The bulkiness and rigidity of the units to which the pendant ionic groups are attached as well as the efficiency of the terminal ionic groups in immobilizing the polymer backbone could explain the trends observed among both the alkyl and ether derivatives. The lower clustering tendency of the ether compounds, compared to the alkyl derivatives, could be rationalized in terms of the solvating effect of the alkyl aryl ether linkage of these ionomers.

Acknowledgment. We are most grateful to Bryn Hird for making the styrene-sodium methacrylate ionomers dynamic mechanical data available to us. Funding for this work was provided by the Natural Sciences and Engineering Research Council of Canada (NSERC) and the U.S. Army Research Office (ARO). M.G. would also like to acknowledge the financial support of NSERC and of the Fonds pour la Formation de Chercheurs et l'Aide á la Recherche (Quebec).

References and Notes

(1) (a) Eisenberg, A.; King, M. *Ion-Containing Polymers*; Academic: New York, 1977. (b) Bazuin, C. G.; Eisenberg, A. *Ind. Eng. Chem. Prod. Res. Dev.* **1981**, *20*, 271. (c) MacKnight, W. J.; Earnest, T. R., Jr. *J. Polym. Sci., Macromol. Rev.* **1981**, *16*, 41. (d) Fitzgerald, J. J.; Weiss, R. A. *J. Macromol. Sci., Rev. Macromol. Chem. Phys.* **1988**, *C28*, 99.

(2) (a) Navratil, M.; Eisenberg, A. *Macromolecules* **1974**, *7*, 84. (b) Makowski, H. S.; Lundberg, R. D.; Westerman, L.; Bock, J. In *Ions in Polymers*; Eisenberg, A., ed.; Advances in Chemistry 187; American Chemical Society: Washington, DC, 1980; pp 3–19.

(3) Brockman, N. L.; Eisenberg, A. *J. Polym. Sci., Polym. Phys. Ed.* **1985**, *23*, 1145.

(4) (a) Lundberg, R. D.; Makowski, H. S. In *Ions in Polymers*; Eisenberg, A., Ed.; Advances in Chemistry 187; American Chemical Society: Washington, DC, 1980; pp 21–36. (b) Rigdahl, M.; Eisenberg, A. *J. Polym. Sci., Polym. Phys. Ed.* **1981**, *19*, 1641.

(5) (a) Gauthier, M. Ph.D. Thesis, McGill University: Montreal, January 1989. (b) Gauthier, M.; Eisenberg, A., submitted for publication in *Macromolecules*.

(6) *Perfluorinated Ionomer Membranes*; Eisenberg, A., Yeager, H. L., Eds.; ACS Symposium Series 180; American Chemical Society: Washington, DC, 1982.

(7) Nafion is a registered trademark of E. I. du Pont de Nemours and Co.

(8) Dow Chemical, U.S. Patent 4 417 969.

(9) Ukihashi, H.; Yamabe, M. In ref 6, p 427. Flemion is a registered trademark of the Asahi Glass Co.

(10) Seko, M.; Ogawa, S.; Kimoto, K. In ref 6, p 365.

(11) Sata, T.; Onoue, Y. In ref 5, p 411. Neosepta-F is a registered trademark of the Tokuyama Soda Co.

(12) See, for example: Hashimoto, T.; Fujimura, M.; Kawai, H. In ref 6, p 217.

(13) (a) Moore, R. B., III; Martin, C. R. *Macromolecules* **1988**, *21*, 1334. (b) Moore, R. B., III; Martin, C. R. *Macromolecules* **1989**, *22*, 3594.

(14) (a) DeMejo, L.; MacKnight, W. J.; Vogl, O. *Polymer* **1978**, *19*, 956. (b) DeMejo, L. P.; MacKnight, W. J.; Vogl, O. *Soc. Plast. Eng., Tech. Pap.* **1978**, *24*, 5. (c) MacKnight, W. J.; DeMejo, L.; Vogl, O. *Acta Polym.* **1980**, *31*, 617. (d) Bansleben, D. A.; Janovic, Z.; Vogl, O. *J. Polym. Sci., Polym. Chem. Ed.* **1984**, *22*, 3263. (e) Bansleben, D. A.; Vogl, O. *J. Polym. Sci., Polym. Chem. Ed.* **1985**, *23*, 703. (f) Muggee, J.; Vogl, O. *J. Polym. Sci., Polym. Chem. Ed.* **1986**, *24*, 2327.

(15) Huiji, L. et al., to be submitted for publication.

(16) (a) Clas, S.-D.; Eisenberg, A. *J. Polym. Sci., Polym. Phys. Ed.* **1986**, *24*, 2743. (b) *Ibid.* **1986**, *24*, 2757.

(17) Gauthier, M.; Eisenberg, A. *J. Polym. Sci., Polym. Chem. Ed.*, in press.

(18) Eisenberg, A.; Navratil, M. *Macromolecules* **1974**, *7*, 90.

(19) Hird, B.; Eisenberg, A. *J. Polym. Sci., Polym. Phys. Ed.*, in press.

(20) Brockman, N. L.; Eisenberg, A. *J. Polym. Sci., Polym. Phys. Ed.* **1985**, *23*, 1145.

(21) *Ionic Polymers*; Holliday, L., Ed.; Applied Science: London, 1975; p 36.

(22) Searles, S., Jr.; Tamres, M. In *The Chemistry of the Ether Linkage*; Patai, S., Ed.; Interscience: New York, 1967; Chapter 6.

(23) Matsuura, H.; Eisenberg, A. *J. Polym. Sci., Polym. Phys. Ed.* **1976**, *14*, 1201.

(24) Rigdahl, M.; Eisenberg, A. *J. Polym. Sci., Polym. Phys. Ed.* **1981**, *19*, 1641.

(25) Weiss, R. A.; Lundberg, R. D.; Turner, S. R. *J. Polym. Sci., Polym. Chem. Ed.* **1985**, *23*, 549.

(26) (a) Hart, H.; Eleuterio, H. S. *J. Am. Chem. Soc.* **1954**, *76*, 519. Elkobaisi, F. M.; Hickinbottom, W. J. *J. Chem. Soc.* **1959**, 1873. (c) See also ref 22, Chapters 4 and 14.

(27) (a) Kenyon, A. S.; Nielsen, L. E. *J. Macromol. Sci., Chem.* **1969**, *A3*, 275. (b) Babayevsky, P. G.; Gillham, J. K. *J. Appl. Polym. Sci.* **1973**, *17*, 2067. (c) Dynes, P. J.; Kaelble, D. H. *J. Appl. Polym. Sci.* **1978**, *22*, 837. (d) Senich, G. A.; MacKnight, W. J.; Schneider, N. S. *Polym. Eng. Sci.* **1979**, *19*, 313.

(28) Lee, C. Y.-C.; Goldfarb, I. J. *Polym. Eng. Sci.* **1981**, *21*, 951.

(29) Bevington, P. R. *Data Reduction and Error Analysis for the Physical Sciences*; McGraw-Hill: New York, 1969; Chapter 6.